[1.] Sanatan PRASAD, [2.] Anant PRASAD

INTEGRAL–LUMP MODEL FOR FREEZING AND MELTING OF AN AGITATED BATH MATERIAL ONTO A LOW MELTING TEMPERATURE SOLID PLATE ADDITIVE

[1.] Mechanical Engineering Department, R.V.S. College of Engineering and Technology, Jamshedpur, INDIA
[2.] Mechanical Engineering Department, National Institute of Technology, Jamshedpur, INDIA

Abstract: The current work involves development of a non–dimensional integral lump model for freezing and melting of agitated bath material around a low melting temperature plate additive and associated heating and melting of the additive. The model exhibits these events dependence upon conduction factor, C_{of}, Phase–change parameter, the Stefan number, S_{ta}, of the additive and melt temperature–ratio, θ_{ab} when the frozen layer thickness, ξ^*_{bm} is taken as frozen layer thickness per unit Stefan number, S_{tb}, of the bath material, $\xi^*_{bm} = (\xi_{bm} - C_r)/S_{tb}$ and the time, τ^* as time per unit property–ratio, $\tau^* = \tau/B$. The model yields closed–form solutions for freezing and melting of bath material, ξ^*_{bm} along with associated heating, ξ^*_{ai} and melting ξ^*_{am} of the additive. Reducing the value of any of the C_{of}, S_{ta} and θ_{ab} decreases the ξ^*_{bm}, ξ^*_{ai} and ξ^*_{am}. For no formation of frozen layer, C_{of} is allowed to decrease the zero value $\tau \to 0$. To validate the model, it is converted to those of literature giving exactly the same expression as of literature.

Keywords: freezing and melting, mathematical modelling, additive melt–bath system

1. INTRODUCTION

Due to increasing competition in the global market, steel makers are required to produce steel and cast iron of various grades at low cost, with enhance productivity and without compromise in their quality and effecting adversely the surrounding environment. To produce them, their melt is made by adding and assimilating an alloyant called additive in hot melt bath and then it is treated by different metallurgical processes before it is cast. Here, freezing and melting of the bath material onto the additive not required in the melt preparation takes place soon after its addition at the surrounding temperature in the bath. It is completed in a certain time and increases the production time and reduces the productivity of such a production. In view of this, decrease in the frozen layer thickness of the bath material and its time of melting is essential. It can be achieved once there is a development of high temperature gradient towards additive side as soon as the additive is ducked in the bath. It requires high conductive heat to be conducted in the additive. This is much more than the convective heat available from the bath. Deficient amount of convective heat needs to be compensated by latent heat of fusion evolved due to freezing of the bath material onto the additive. If the bath is agitated it increases much the availability of the convective heat. As a result, only a small amount of latent heat of fusion is required to balance the conductive heat.

It is provided by developing a thin layer of the frozen layer onto the additive. The freezing of this layer with its subsequent melting takes much less time resulting in diminishing the production time and increasing the productivity.

Study of such a happening for a low melting temperature plate additive seldom appears in the literature. However, freezing and melting of the agitated bath material onto the high melting temperature plate [1], cylinder [2], spherical [3] and low melting temperature cylindrical [4] additive were investigated. Solutions for such types of freezing and melting onto these additives were obtained in closed form. Closed–form solutions for the freezing and melting of the bath material onto the temperature dependent heat capacity plate additive having high melting temperature a negligible thermal resistance with respect to the bath was also reported [5]. Recently, for highly agitated bath and high melting temperature melt superheat [6] frozen layer development around DRI spherical particle was obtained. It took 50% of total time of melting of such a particle. In this situation, there was almost no formation of frozen layer. In case the particle size or the particle initial temperature was increased, the frozen layer development and the melting time of the particle were increased. Moreover, increase in heat capacity or decrease in the thermal conductivity of the particle of the particle increases particle melting time.

2. FORMATION OF PROBLEM

To model mathematically undesirable freezing and melting of a bath material onto an additive just after dunking it in a hot melt bath, a low melting temperature plate additive of semi thickness, b at an initial

ISSN 1584 – 2665 (printed version); ISSN 2601 – 2332 (online); ISSN-L 1584 – 2665

temperature T_{ai} less than its melting temperature T_{am} ($T_{ai} < T_{am}$) is considered. It is immersed in a hot melt bath maintained at a uniform temperature, T_b greater than the freezing temperature, T_{bm} of the bath material which is also greater than the melting temperature, T_{am} of the additive.

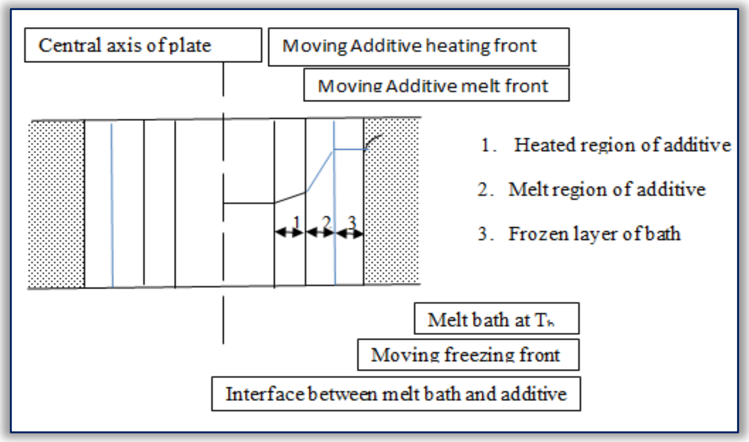

Figure 1. Freezing of the bath material

Immediately freezing of the bath material onto the Figure1: Schematic diagram of freezing and melting of bath material around a solid plate additive immersed in the agitated bath additive and heating and melting of the additive set in and the interface formed between the freezing of bath material onto the additive and melting of the additive attains an equilibrium temperature T_e that lies between T_{am} and T_{bm}. Moreover, the temperature gradient on the additive and the frozen layer sides are developed along with the establishment of temperature field $T_{ai}<T_{am}<T_e<T_{bm}<T_b$ in the additive–melt bath System, Figure1. Passing of the time allows the growth of the frozen layer thickness onto the additive, increase in the melt depth and the heat penetration thickness in the additive and rise in the interface temperature T_e. These happenings continue till the requirement of the conductive heat by the additive due to high temperature gradient on its side is more than the convective heat supplied by the melt bath. For thermal equilibrium, the excess of the conductive heat is met by the latent heat of fusion generated due to freezing of the bath material onto the additive. After this time, the bath convective heat becomes more than the conductive heat needed by the additive resulting in the melting of the frozen layer completely exposing the additive in melted and heated state with the additive melt layer gets detached and assimilates in the bath.

This event is axisymmetric and conduction controlled. The melting of the additive is represented by integral form of non–dimensional heat conduction equation

$$B\frac{d}{d\tau}\int_{\xi_{am}}^{1}\theta_{af}\xi_{af} - \theta_{af}\Big|_{\xi_{af}=1}\frac{d1}{d\tau} + \theta_{af}\Big|_{\xi_{af}=\xi_{am}}\frac{d\xi_{am}}{d\tau} = \frac{\partial\theta_{af}}{\partial\xi_{af}}\Big|_{\xi_{af}=1} - \frac{\partial\theta_{af}}{\partial\xi_{af}}\Big|_{\xi_{af}=\xi_{am}} \tag{1}$$

Its related initial and boundary conditions are

$$\theta_{af} = 0\ ,\ -1 \le \xi_{af} \le +1,\ \tau = 0 \tag{2}$$

$$\theta_{af} = \theta_e > \theta_{ab},\ \xi_{af} = 1,\ \tau > 0 \tag{3}$$

$$\theta_{af} = \theta_{ab},\ \xi_{af} = \xi_{am},\ \tau > 0 \tag{4}$$

The heating of the additive is governed by integral form of the non–dimensional heat conduction equation

$$B\frac{d}{d\tau}\int_{\xi_{ai}}^{\xi_{am}}\theta_{ah}\xi_{ah} - \theta_{ah}\Big|_{\xi_{ah}=\xi_{am}}\frac{d\xi_{am}}{d\tau} + \theta_{ah}\Big|_{\xi_{ah}=\xi_{ai}}\frac{d\xi_{ai}}{d\tau} = \frac{\partial\theta_{ah}}{\partial\xi_{ah}}\Big|_{\xi_{ah}=\xi_{am}} - \frac{\partial\theta_{ah}}{\partial\xi_{ah}}\Big|_{\xi_{ah}=\xi_{ai}} \tag{5}$$

Its associated initial and boundary conditions take, respectively, the following form

$$\theta_{ah} = 0,\ -1 \le \xi_{ah} \le 1,\ \tau = 0 \tag{6}$$

$$\theta_{ah} = \theta_{ab},\ \xi_{ah} = \xi_{am},\ \tau > 0 \tag{7}$$

$$\theta_{ah} = 0,\ \frac{\partial\theta_{ah}}{\partial\xi_{ah}} = 0,\ \xi_{ah} = \xi_{ai},\ \tau > 0 \tag{8}$$

The coupling conditions between melting and heating of the additive are

ISSN 1584 – 2665 (printed version); ISSN 2601 – 2332 (online); ISSN-L 1584 – 2665

$$\theta_{ah} = \theta_{af} = \theta_{ab}, \;\; \xi_{ah} = \xi_{af} = \xi_{am}, \;\; \tau > 0 \tag{9}$$

$$\frac{\partial\theta_{af}}{\partial\xi_{af}} + \frac{B}{S_{ta}}\frac{d\xi_{am}}{\partial\tau} = \frac{\partial\theta_{ah}}{\partial\xi_{ah}}, \;\; \xi_{ah} = \xi_{af} = \xi_{am}, \;\; \tau > 0 \tag{10}$$

As stated in the introduction, the highly agitated bath develops a thin frozen layer of the bath material on to the immerged plate additive.Its thermal resistance is negligible with respect to that of the additive leading to establishment of uniform temperature in the entire frozen layer thickness. This temperature is the freezing temperature, T_{bm} of the bath material because the advancing frozen layer is at this freezing temperature, T_{bm}. This permits the interface between the additive and the freezing layer also at this freezing temperature, T_{bm}. This makes $\theta_e = 1$. Also, these features make the thin layer a lump that does not liberate or absorb the sensible heat.

Employing an energy balance between the heat conducted to the additive with sum of the heat evolved due to the freezing of the bath material onto the additive and the bath convective heat leads to

$$\frac{1}{BC_{of}} + \frac{1}{S_{tb}}\frac{d\xi_{bm}}{d\tau} = -Q_{bn}, \;\; \xi_{bf} = \xi_{bm}, \tag{11}$$

Its initial condition is

$$\xi_{bf} = C_r = 1, \qquad \tau = 0 \tag{12}$$

The coupling conditions at the interface between the freezing layer of the bath material and melting layer of the additive are

$$\frac{1}{B}\frac{\partial\theta_{af}}{\partial\xi_{af}} = -Q_{bn}; \quad \text{and } \theta_{af} = \theta_{bf} = \theta_e = 1, \quad \xi_{af} = 1, \;\; \xi_{bf} = C_r, \;\; \tau > 0 \tag{13}$$

3. SOLUTION

Equations (1) to (13) represented a non–dimensional lump integral form of mathematical model of the current event. The model assumes of thermo–physical properties of the melt layer and the heated portion of the additive uniform and the same whereas those of the frozen layer and the additive are uniform but different. The change in the volume of the additive upon heating and melting is taken to be negligible and the surface of the additive is assumed to be in perfect contact with the surface of the freezing layer due to the occurrence of negligible interface thermal resistance ranging from $1.9\text{x}10^{-4}$ m^2sK/J to $2.1\text{x}10^{-4}$ m^2sK/J [7] between them. In the earlier studies [8–24] this assumption yielded accurate and realistic results. Also, the low melting temperature additive remains within the frozen layer developed until the frozen layer melts completely allowing the detachment of the melt layer of the additive that assimilates in the melt bath.

Employing Eqs.(3) and (4), Eq.(1) related to melting of the additive reduces to

$$B\frac{d}{d\tau}\int_{\xi_{am}}^{1}\theta_{af}d\xi_{af} + \theta_{ab}\frac{d\xi_{am}}{d\tau} = \left.\frac{\partial\theta_{af}}{\partial\xi_{af}}\right|_{\xi_{af}=1} - \left.\frac{\partial\theta_{af}}{\partial\xi_{af}}\right|_{\xi_{af}=\xi_{am}}. \tag{14}$$

whereas Eq.(5) associated with heating of the additive changes to

$$B\frac{d}{d\tau}\int_{\xi_{ai}}^{\xi_{am}}\theta_{ah}d\xi_{ah} - \theta_{ab}\frac{d\xi_{am}}{d\tau} = \left.\frac{\partial\theta_{ah}}{\partial\xi_{ah}}\right|_{\xi_{hf}=\xi a_m}. \tag{15}$$

once Eqs. (7) and (8) are applied. Addition of Eqs. (14) and (15) gives a globalized equation

$$B\frac{d}{d\tau}\left[\int_{\xi_{ai}}^{\xi_{ah}}\theta_{ah}d\xi_{ah} + \int_{\xi_{am}}^{1}\theta_{af}\xi_{af}\right] = \left.\frac{\partial\theta_{af}}{\partial\xi_{af}}\right|_{\xi_{af}=1} - \left.\frac{\partial\theta_{af}}{\partial\xi_{af}}\right|_{\xi_{af}=\xi_{am}} + \left.\frac{\partial\theta_{ah}}{\partial\xi_{ah}}\right|_{\xi_{ah}=\xi_{am}} \tag{16}$$

Employing Eq.(10), Eq.(16) is further reduced to

$$B\frac{d}{dt}\left[\int_{\xi_{ai}}^{\xi_{am}}\theta_{ah}d\xi_{ah} + \int_{\xi_{am}}^{1}\theta_{af}d\xi_{af}\right] = \left.\frac{\partial\theta_{af}}{\partial\xi_{af}}\right|_{\xi_{af}=1} - \frac{B}{S_{ta}}\frac{d\xi_{am}}{d\tau} \tag{17}$$

To find the solution of the globalized Eq.(17), the temperature distributions both in the melt region and the heated region of the additive need to be prescribed.

A linear temperature profile in the melt region that satisfies Eqs. (3) and (4) is assumed as

ISSN 1584 – 2665 (printed version); ISSN 2601 – 2332 (online); ISSN-L 1584 – 2665

$$\theta_{af} = \theta_e - (\theta_e - \theta_{ab})\left(\frac{1-\xi_{af}}{1-\xi_{am}}\right). \tag{18}$$

whereas in the heated layer of the additive a cubic temperature distribution is taken

$$\theta_{ah} = \theta_{ab}\left(\frac{\xi_{ah} - \xi_{ai}}{\xi_{am} - \xi_{ai}}\right)^3. \tag{19}$$

It fulfils Eqs. (7) and (8).
Note that in the previous studies choice of a linear temperature profile, Eq.(19) in the melting [27–30] and freezing [8,24,25] problems yielded accurate results whereas a cubic temperature distribution in Eq.(19) in the heating problems [31,32] provided results close to exact solutions [33].
Employing Eqs. (18) and (19), Eq.(17) gives

$$B\left[\frac{d}{d\tau}\left\{\frac{\theta_{ab}}{4}(\xi_{am} - \xi ai)\right\} + \theta_e(1-\xi_{am}) - \frac{(\theta_e - \theta_{ab})}{2}(1-\xi_{am})\right] = \frac{(\theta_e - \theta_{ab})}{(1-\xi_{am})} - \frac{B}{S_{ta}}\frac{d\xi_{am}}{d\tau}. \tag{20}$$

It is re–arranged as

$$\left[\frac{d}{d\tau}\left\{\frac{\theta_{ab}}{4}(\xi_{am} - \xi_{ai})\right\} + \frac{(\theta_e + \theta_{ab})}{2}(1-\xi_{am}) + \frac{1}{S_{ta}}\xi_{am}\right] = \frac{(\theta_e - \theta_{ab})}{B(1-\xi_{am})}. \tag{21}$$

whereas Eq.(10) takes the form

$$\frac{\theta_e - \theta_{ab}}{1-\xi_{am}} + \frac{B}{S_{ta}}\frac{d\xi_{am}}{d\tau} = \frac{3\theta_{ab}}{\xi_{am} - \xi_{ai}}. \tag{22}$$

The conjugating condition, Eq.(13) at the interface between the freezing layer of the bath material and the melt layer of the additive becomes

$$\frac{\theta_e - \theta_{ab}}{B(1-\xi_{am})} = -Q_{bm} \tag{23}$$

once Eq.(18) applied to it. Substitution of Eq.(23), Eq.(11) becomes

$$\frac{1}{BC_{of}} + \frac{1}{S_{tb}}\frac{d\xi_{bm}}{d\tau} = \frac{\theta_e - \theta_{ab}}{B(1-\xi_{am})} \tag{24}$$

Equating Eq.(21) with Eq.(24) gives

$$\left[\frac{d}{d\tau}\left\{\frac{\theta_{ab}}{4}(\xi_{am} - \xi_{ai})\right\} + \frac{(\theta_e + \theta_{ab})}{2}(1-\xi_{am}) + \frac{\xi_{am}}{S_{ta}}\right] = \frac{1}{BC_{of}} + \frac{1}{S_{tb}}\frac{d\xi_{bm}}{d\tau}. \tag{25}$$

Its re–arranged form becomes

$$\left[\frac{d}{d\tau}\left\{\frac{\theta_{ab}}{4}(\xi_{am} - \xi_{ai})\right\} + \frac{(\theta_e + \theta_{ab})}{2}(1-\xi_{am}) + \frac{\xi_{am}}{S_{ta}} - \frac{\xi_{bm}}{S_{tb}}\right] = \frac{1}{BC_{of}}. \tag{26}$$

Satisfying the conditions $\xi_{bm} = C_r$, $\xi_{am} = \xi_{ai} = 1$ at $\tau = 0$ Eq.(26) leads to a closed–form solution

$$\frac{\tau}{BC_{of}} = \frac{\theta_{ab}}{4}(\xi_{am} - \xi_{ai}) + \frac{(\theta_e - \theta_{ab})}{2}(1-\xi_{am}) - \frac{1-\xi_{am}}{S_{ta}} - \frac{1-\xi_{bm}}{S_{tb}} \tag{27}$$

Assuming $\frac{\xi_{bm} - C_r}{S_{tb}} = \xi^*{}_{bm}$, $\frac{\tau}{B} = \tau^*$

Eq.(27) tranforms to

$$\xi^*{}_{bm} = -\frac{\tau^*}{C_{of}} + \left[\left\{\frac{\theta_{ab}}{4}(\xi_{am} - \xi_{ai})\right\} + \left(\frac{\theta_e + \theta_{ab}}{2} - \frac{1}{S_{ta}}\right)(1-\xi_{am})\right] \tag{28}$$

As explained earlier, the interface temperature θ_e between the frozen layer of the bath material and the melt of the additive that appears in Eqs. (22) to (28) is, the freezing temperature of bath material $(\theta_e = 1)$. Its application makes Eqs. (22), (24) and (28), respectively, as

ISSN 1584 – 2665 (printed version); ISSN 2601 – 2332 (online); ISSN-L 1584 – 2665

$$\frac{1-\theta_{ab}}{1-\xi_{am}}+\frac{B}{S_{ta}}\frac{d\xi_{am}}{d\tau}=\frac{3\theta_{ab}}{\xi_{am}-\xi_{ai}}. \tag{29}$$

$$\frac{1}{BC_{of}}+\frac{1}{S_{tb}}\frac{d\xi_{bm}}{d\tau}=\frac{1-\theta_{ab}}{B(1-\xi_{am})} \tag{30}$$

$$\xi^*{}_{bm}=-\frac{\tau^*}{C_{of}}+\left[\left\{\frac{\theta_{ab}}{4}(\xi_{am}-\xi_{ai})\right\}+\left(\frac{1+\theta_{ab}}{2}-\frac{1}{S_{ta}}\right)(1-\xi_{am})\right] \tag{31}$$

To obtain closed–form solutions for the melt depth ξ_{am} and the heat penetration depth ξ_{ai} in the additive Eq.(29) needs to be solved but it does not provide closed–form solution due to the presence of $d\xi_{am}/d\tau$ in it. To overcome this difficulty $d\xi_{am}/d\tau$ is required to be transformed to an algebraic expression. To obtain its total differential of the temperature $\theta_{ah}=\theta_{ah}[\xi_{ah}(\tau),\tau]$, at the interface $\xi_{ah}=\xi_{am}$ between the melt layer and heating layer of the additive is zero due to $\theta_{ah}=\theta_{ah}$ at $\xi_{ah}=\xi_{am}$

$$\frac{D\theta_{ah}}{D\tau}=\frac{\partial\theta_{ah}}{\partial\tau}\frac{\partial\xi_{ah}}{d\tau}+\frac{\partial\theta_{ah}}{\partial\tau}=0 \tag{32}$$

giving

$$\left.\frac{d\xi_{ah}}{d\tau}\right|_{\xi_{ah}=\xi_{ami}}=-\frac{\left.\frac{\partial\theta_{ah}}{\partial\tau}\right|_{\xi_{ah}=\xi_{am}}}{\left.\frac{\partial\theta_{ah}}{\partial\xi_{ah}}\right|_{\xi ah=\xi am}}\quad \text{at } \xi_{ah}=\xi_{am} \tag{33}$$

In the heated region of the additive, the differential form of heat conduction equation in place of in place of integral form Eq. (5) becomes $\frac{\partial\theta_{ah}}{\partial\tau}=\frac{1}{B}\frac{\partial^2\theta_{ah}}{\xi_{ah}{}^2}$

Its application to Eq.(33) leads to

$$\left.\frac{d\xi_{ah}}{d\tau}\right|_{\xi_{ah}=\xi_{am}}=-\frac{1}{B}\left.\frac{\frac{\partial\theta^2{}_{ah}}{\partial\xi^2{}_{ah}}}{\frac{\partial\theta_{ah}}{\partial\xi_{ah}}}\right|_{\xi_{ah}=\xi_{am}} \tag{34}$$

Using Eq.(19), it gets converted to

$$\frac{d\xi_{am}}{d\tau}=-\frac{1}{B}\frac{\frac{6\theta_{ab}}{(\xi_{am}-\xi_{ai})^2}}{\frac{3\theta_{ab}}{(\xi_{am}-\xi_{ai})}}=-\frac{2}{B(\xi_{am}-\xi_{ai})}. \tag{35}$$

Combination of Eq. (29) and Eq. (35) gives

$$\frac{1-\theta_{ab}}{1-\xi_{am}}+\frac{1}{S_{ta}}\frac{2}{\xi_{am}-\xi_{ai}}=\frac{3\theta_{ab}}{\xi_{am}-\xi_{ai}}. \tag{36}$$

It leads to

$$\xi_{am}-\xi_{ai}=\frac{(3\theta_{ab}S_{ta}+2)}{(1-\theta_{ab})S_{ta}}(1-\xi_{am})=S_{tm}(1-\xi_{am}),\ \text{here, } \frac{(3\theta_{ab}S_{ta}+2)}{(1-\theta_{ab})S_{ta}}=S_{tm} \tag{37}$$

Substitution of Eq.(37) in Eq.(31) makes it

$$\xi^*{}_{bm}=-\frac{\tau^*}{C_{of}}+\left[\frac{\theta_{ab}S_{tm}}{4}+\left(\frac{1+\theta_{ab}}{2}-\frac{1}{S_{ta}}\right)(1-\xi_{am})\right] \tag{38}$$

Eq.(38) is reduced to

ISSN 1584 – 2665 (printed version); ISSN 2601 – 2332 (online); ISSN-L 1584 – 2665

$$\xi^*_{bm} = -\frac{\tau^*}{C_{of}} + S_{tmn}\left(1-\xi_{am}\right), \text{ where } S_{tmn} = \left[\frac{\theta_{ab}S_{tm}}{4} + \left(\frac{1+\theta_{ab}}{2} - \frac{1}{S_{ta}}\right)\right] \tag{39}$$

Using Eq.(37), Eq.(21) is transformed to

$$\frac{d}{d\tau}\left[S_{tmp}\left(1-\xi_{am}\right) - \frac{\xi_{am}}{S_{ta}}\right] = \frac{\left(1-\theta_{ab}\right)}{B\left(1-\xi_{am}\right)} \text{ where } S_{tmp} = \frac{\theta_{ab}S_{tm}}{4} + \frac{\left(1-\theta_{ab}\right.}{2} \tag{40}$$

It is further transformed to

$$\frac{d}{d\tau}\left[\left(S_{tmp} + \frac{1}{S_{ta}}\right)\left(1-\xi_{am}\right) - \frac{1}{S_{ta}}\right] = \frac{\left(1-\theta_{ab}\right)}{B\left(1-\xi_{am}\right)} \tag{41}$$

On application of $S_{tmp} + \frac{1}{S_{ta}} = S_t^*$ and $1-\xi_{am} = \xi^*_{am}$, Eq.(41) takes the form

$$\frac{d}{d\tau}\left[S_t^*\xi^*_{am} - \frac{1}{S_{ta}}\right] = \frac{\left(1-\theta_{ab}\right)}{B\xi^*_{am}}. \tag{42}$$

It readily gives a closed–form solution for the melt depth ξ^*_{am} in the additive

$$\xi^*_{am} = \left(1-\xi_{am}\right) = \sqrt{\frac{2\left(1-\theta_{ab}\right)}{S_t^*}\frac{\tau}{B}} = \sqrt{\frac{2\left(1-\theta_{ab}\right)}{S_t^*}\tau^*}, \; \tau^* = \frac{\tau}{B}, \tag{43}$$

For heated depth of additive Eq.(37) is rearranged as

$$(1-\xi_{ai}) - (1-\xi_{am}) = S_{tm}\left(1-\xi_{am}\right) \tag{44}$$

It becomes

$$(1-\xi_{ai}) = \left(1+S_{tm}\right)\left(1-\xi_{am}\right) \tag{45}$$

Using Eq.(43), Eq.(45) takes the form

$$\left(1-\xi_{ai}\right) = \xi^*_{ai} = \left(1+S_{tm}\right)\sqrt{\frac{2\left(1-\theta_{ab}\right)}{S_t^*}\tau^*}, \tag{46}$$

whereas Eq.(39) becomes

$$\xi^*_{bm} = -\frac{\tau^*}{C_{of}} + S_{tmn}\sqrt{\frac{2\left(1-\theta_{ab}\right)}{S_t^*}\tau^*}, \tag{47}$$

It may be noted that Eq.(47), Eq.(46) and Eq.(45) give closed form solutions respectively for frozen layer thickness, ξ^*_{bm}, the melt depth, ξ^*_{am} and the heat penetration depth ξ^*_{ai} in the additive.

Maximum frozen layer thickness development and its time of growth:

To obtain the growth the maximum frozen layer thickness, $\frac{d\xi_{bm}}{d\tau} = 0$ and $\frac{d^2\xi_{bm}}{d\tau^2} \leq 0$.

Using Eq.(47)

$$\frac{d^*\xi_{bm}}{d\tau} = -\frac{1}{C_{of}} + S_{tmn}\sqrt{\frac{2\left(1-\theta_{ab}\right)}{S_t^*}}\frac{1}{2\sqrt{\tau^*}} = 0,$$

giving

$$\tau^* = \frac{1}{2}C_{of}^{\;2}S_{tmn}^{\;2}\left(\frac{1-\theta_{ab}}{S_t^*}\right) \tag{48}$$

Applying this condition satisfies the condition for the growth of the maximum frozen layer thickness $\frac{d^2\xi_{bm}}{d\tau^2} \leq 0$. As a result, Eq.(48) denotes the time for the growth of the maximum frozen layer thickness represented by τ^*_{max} and Eq.(48) can be written as

$$\tau^*_{max} = \frac{1}{2}C_{of}^{\;2}S_{tmn}^{\;2}\left(\frac{1-\theta_{ab}}{S_t^*}\right) \tag{49}$$

ISSN 1584 – 2665 (printed version); ISSN 2601 – 2332 (online); ISSN-L 1584 – 2665

Substituting it in Eq.(47) gives the expression for the maximum frozen layer thickness

$$\xi^*_{bmx} = \frac{1}{2}\frac{S^2_{tmn}}{S^*_t}(1-\theta_{ab})C_{of} \tag{50}$$

Total time, τ^*_t of Freezing and Melting:

When freezing and melting, ξ^*_{bm} becomes zero $(\xi^*_{bm} = 0)$, the time τ^* required for this is the total time τ^*_t. Substituting it makes Eq.(47)

$$\xi^*_{bm} = 0 = -\frac{\tau^*_t}{C_{of}} + S_{tmn}\sqrt{\frac{2(1-\theta_{ab})}{S^*_t}\tau^*_t},$$

It gives

$$\tau^*_t = 2C^2_{of}S^2_{tmn}\frac{(1-\theta_{ab})}{S^*_t} \tag{51}$$

Time of Melting, τ^*_{mel}:

Subtracting Eq.(49) from Eq.(51) provides the melting time of the frozen layer developed. It becomes

$$\tau^*_{mel} = \frac{3}{2}C_{of}{}^2S_{tmn}{}^2\left(\frac{1-\theta_{ab}}{S^*_t}\right) \tag{52}$$

Using Eq.(49), Eq.(52) becomes $\tau^*_{mel} = 3\tau^*_{max}$. It states that frozen layer time τ^*_{max} takes three times of melting time τ^*_{mel}.

Time for Heat Penetration Reaching the Central Axis of the Additive:

Here, ξ_{ai} reaches the central axis $(\xi_{ai} = 0)$. In this situation, the melt depth in the additive and the frozen layer thickness can be obtained. Employing Eq.(46) gives time for $\xi_{ai} = 0$.

$$\tau^* = S_t^* / \left\{2(1-\theta_{ab})(1+S_{ta})^2\right\} \tag{53}$$

The melt depth in the additive in this situation takes the form

$$\xi^*_{am} = 1/(1+S_{ta})^2 \tag{53a}$$

Once Eq.(44) is applied to Eq.(53),

Whereas the frozen layer thickness becomes

$$\xi^*_{bm} = -\frac{S^*_t}{2C_{of}(1-\theta_{ab})(1+S_{tm})^2} + \frac{S^*_{tm}}{(1+S^*_{tm})}, \tag{53b}$$

when Eq.(53) is substituted to Eq.(47),

At the time, τ^*_t for the complete melting of the frozen layer, the melt depth of the additive, Eq.(44) becomes

$$\xi^*_{amt} = \sqrt{\frac{2(1-\theta_{ab})}{S^*_t}C^2_{of}S^2_{tmn}\frac{(1-\theta_{ab})}{S^*_t}} = \frac{2}{S^*_t}(1-\theta_{ab})C_{of}S_{tmn} \tag{54}$$

And the heat penetration depth in the additive, Eq.(46) becomes

$$\xi^*_{ait} = (1+S_{tm})\sqrt{\frac{2(1-\theta_{ab})}{S^*_t}2C^2_{of}S^2_{tmn}\frac{(1-\theta_{ab})}{S^*_t}} = \frac{2}{S^*_t}(1+S_{tmn})(1-\theta_{ab})C_{of}S_{tmn} \tag{55}$$

4. VALIDITY

In case the plate additive melting temperature is higher than the bath material freezing temperature, no melting of the additive takes place and there is no melt layer of the additive.

This results in vanishing Eq.(1) coupling condition Eq.(8) and (9) and making $\xi_{ab} = 1$. Employing them reduces Eq.(5) to

$$B\frac{d}{d\tau}\int_{\xi_{ai}}^{1}\theta_{ah}\xi_{ah} - \theta_{ah}\Big|_{\xi ah=1}\frac{d1}{d\tau} + \theta_{ah}\Big|_{\xi_{ah}=\xi_{ai}}\frac{d\xi_{ai}}{d\tau} = \frac{\partial\theta_{ah}}{\partial\xi_{ah}}\Big|_{\xi_{ah}=\xi_{am}} - \frac{\partial\theta_{ah}}{\partial\xi_{ah}}\Big|_{\xi ah=1} \tag{56}$$

ISSN 1584 – 2665 (printed version); ISSN 2601 – 2332 (online); ISSN-L 1584 – 2665

whereas associated initial and boundary conditions remains same as Eq.(6) to Eq.(8) except Eq.(7) I which $\theta_{ah} = 1$

Eq.(56) is reduced to

$$B\frac{d}{d\tau}\int_{\xi_{ai}}^{1}\theta_{ah}\xi_{ah} = -\frac{\partial\theta_{ah}}{\partial\xi_{ah}}\Big|_{\xi ah=1} \tag{57}$$

Once Eqs.(7) and (8) are applied to it. To solve Eq.(57) the temperature distribution in the heated region Eq.(20) needs to be taken with θ_{ab} =1.

$$\theta_{ah} = \left(\frac{\xi_{ab} - \xi_{ai}}{1 - \xi_{ai}}\right)^3 . \tag{58}$$

Employing Eq.(58) in Eq.(57) readily gives a close form solution for heat penetration dept ξ_h

$$(1 - \xi_{ai}) = \xi_h = \sqrt{\frac{24\tau}{B}} \tag{59}$$

It satisfies the initial condition $\xi_{ai} = 1$ at $\tau = 0$, t_h denotes the heat penetration depth in the additive. Note that Eq.(59) is exactly the same as obtained previously [26] for the plate additive thus validating the current problem.

5. RESULT AND DISCUSSIONS

The current study relates the freezing and melting of an agitated bath material onto a low melting temperature plate additive. Its non–dimensional lump–integral model is devised showing this event dependence upon non–dimensional independent parameters; the phase change–parameters, the Stefan number of the bath material, S_{tb} and that of the additive, S_{ta}, the bath condition denoted by the conduction factor, C_{of} , the property–ratio, B, the capacity– ratio, C_r and the melting temperature–ratio, θ_{ab} of the additive bath system. This model also

Table–1: Based on thermo physical properties of the Steel bath [19]
T_b = 1873K(1600 °C) , T_{bm} = 1804K(1531°C), C_b=0.69KJ/KgK, L_{bm} = 277000 J/Kg,
K_{bm}= 29.3W/mK, ρ_{bm} =7820Kg/m³, S_{tb} = 3.751

	Thermo–physical properties of low melting temperature cylindrical solid additive [34] [T_{ai}=298K(25°C), r_0=0.025m]						Non–dimensional parameters		
Additive	T_{am} [K(°C)]	C_{pa} KJ/KgK	ρ_a Kg/m³	L_a KJ/Kg	K_a * W/mK	h w/m²K	S_{ta}	θ_{ab}	C_{of}
Tin	504.9(231.9)	0.226	7300	60.71	60.47	20x10⁴	5.60	0.137	0.288
Bismuth	544.4(271.4)	0.13	9780	51.9	8.0	20x10⁴	3.51	0.16	0.034
Selenium	494(221)	0.352	4816	68.62	0.52	0.25x10⁴	7.72	0.13	0.181
Sulphur	388.2(115.2)	0.71	2000	115.6	0.205	1.2x10⁴	9.25	0.059	0.071

- Data for Ka are taken from Ref [34] and [35].

gives close–form solutions in terms of these independent parameters for the freezing of the bath material ξ_{bm} and related melting ξ_{am} and heating ξ_{ai} of the additive, but when the frozen layer ξ_{bm} is taken as per unit Stefan number S_{tb} of the bath material, as $\xi^*_{bm} = (\xi_{bm} - C_r)/S_{tb}$ and the time per unit property–ratio, B as $\tau^* = \tau/B$,it becomes in terms of only C_{of}, S_{ta} and θ_{ab} . The values of these parameters for various additive–bath systems often employed in industries are tabulated in Table–1. From physical point of views, the conduction factor, C_{of} , represents the ratio of heat conducted to the additive due to the difference of freezing temperature of the bath material and the initial temperature of the additive and convective heat provided by the bath. It lies between zero and infinity ($0 \le C_{of} \le \infty$). $C_{of} \to 0$ is indicative of no heat conducted to the additive owing to which freezing does not take place. In turn, the freezing and melting event is absent. Such an event is achieved once the additive is heated to the freezing temperature of the bath material by its dunking in the bath. $C_{of} \to 0$ is also attained in case of the bath is made highly agitated giving heat transfer co–efficient, ($h \to \infty$). $C_{of} \to \infty$ denotes the absence of convective heat. It is a result of the bath material maintained at its freezing temperature. In this situation, the conductive heat to the additive is balanced by only the latent heat of fusion of the bath material generated owing to the freezing

ISSN 1584 – 2665 (printed version); ISSN 2601 – 2332 (online); ISSN-L 1584 – 2665

of the bath material onto the additive. The freezing continues till it gives latent heat of fusion to balance the conductive heat. The property–ratio, B is the ratio of effusivity, K_bC_b of the bath material and the effusivity, K_aC_a of the additive.It signifies the thermal force. Its high value is indicative of developing small thermal force due to which a large thickness of the frozen layer onto the additive is formed. The melting temperature–ratio, $\theta_{ab} < 1$ of the additive bath system represents the additive melting temperature is less than the bath material freezing temperature. Here, both melting and heating of the additive take place. The heat capacity–ratio, C_r is defined as the ratio of heat capacity C_b of the bath material and that of the additive, C_a, $(C_r = C_b / C_a)$. C_r<1 is indicative of storing large heat in the additive than that in the bath. The phase–change parameters, the Stefan number of the bath material, S_{tb} is the ratio of the sensible heat and the latent heat of fusion of the bath material. When its value is small, it yields large latent heat of fusion due to which a smaller frozen layer thickness is developed onto the additive or a smaller thickness of the additive melts.

Exhibited in Figure2 is time dependent frozen layer, ξ^*_{bm} development onto the additive, melt layer thickness ξ^*_{am} and heat penetration depth ξ^*_{ai} in the additive for various C_{of} with θ_{ab} and S_{ta} are assumed to be parameters, whereas in Figure3 these are plotted for different S_{ta} with θ_{ab} and C_{of} taken as parameter. Figure4 exhibits these plots for various θ_{ab}. Here, C_{of} and S_{ta} are taken as parameters. All these figures show a parabolic behaviour for freezing and melting. The apex of the parabola represents the growth of frozen layer to a maximum extent. The distance between the foot of the apex and the beginning of the frozen layer development denotes the time of the development of the maximum frozen layer thickness whereas feet of the parabola provides the total time of freezing and melting. Also, the frozen layer growth is faster than its melting and takes 33.3% of the time of freezing and melting. The melting of frozen layer is completed in 66.7% of the time of freezing and melting. The ratio of these two times is 3:4 as against 1:4 in case of freezing and melting time of the bath material onto a high melting temperature cylindrical additive [2]. Note that in earlier studies of freezing and melting onto high melting temperature plate and cylindrical additive, similar results were reported

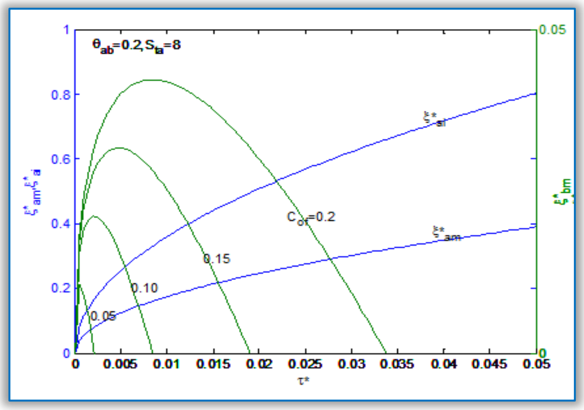

Figure 2: Time variant freezing and melting of the bath material onto the additive and the corresponding melt depth and heat penetration depth in the additive for different conduction factors, C_{of}. θ_{ab} and S_{ta} of the additive are taken as parameters.

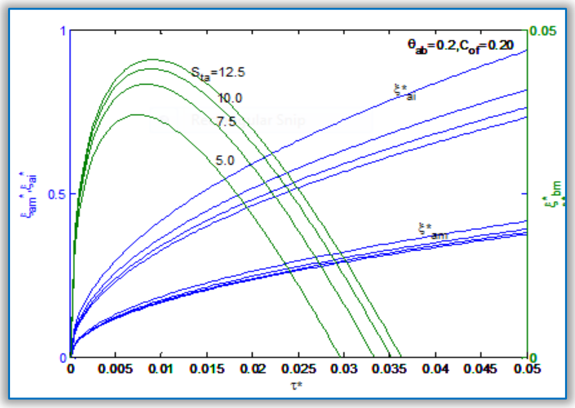

Figure 3: Behaviour of freezing and melting of the bath material onto the additive and the corresponding melt depth and heat penetration depth in the additive for different S_{ta} conduction factor, C_{of} and melting temperature–ratios, θ_{ab} are assumed to be parameters.

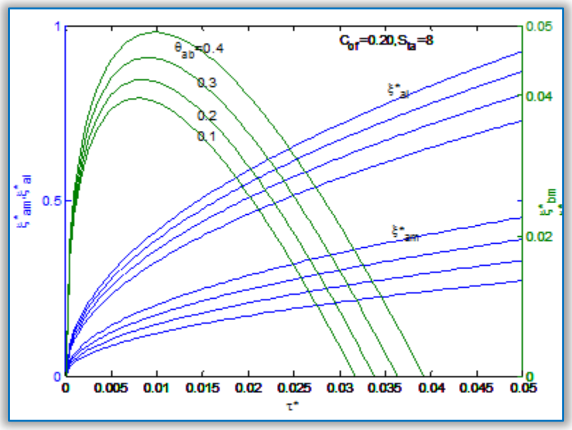

Figure 4: Time dependent freezing and melting of the bath material onto the additive and the corresponding melt depth and heat penetration depth in the additive for different Stefan number, S_{ta}, C_{of}. and θ_{ab} are taken as parameters.

ISSN 1584 – 2665 (printed version); ISSN 2601 – 2332 (online); ISSN-L 1584 – 2665

Influence of Conduction Factor, C_{of} :

Figure(2) relates to time dependent freezing and melting of bath material, ξ^*_{bm} and associated heating, ξ^*_{ai} and melting ξ^*_{am} of the additive. For various values of C_{of}. The Stefan number, S_{ta}, of the additive and melt temperature ratio, θ_{ab} are taken as parameters. It is observed that freezing and melting is parabolic whereas additive heating and melting grow faster in the initial time of development of the frozen layer which subsequently take linear behavior. Decreasing C_{of} from 0.03 to 0.005 reduces the size of parabola and time of freezing and melting. Such a trait seems to be true since decreasing C_{of} increases the bath convective heat and diminishes the requirement of latent heat of fusion of freezing layer to balance the conductive heat needed by the additive. It results in formation of smaller frozen layer thickness.

In Figure(5) conduction factor, C_{of} dependent maximum frozen layer built–up ξ^*_{bmx}, its time of formation, $\tau^*_{\max}$ and its melting time, τ^*_{mel} and total time of freezing and melting τ^*_t are plotted for prescribed θ_{ab} and S_{ta}. It is observed that all these increase as C_{of} increases. Such trends appears to be correct since increasing C_{of} reduces the bath convective heat due to which latent heat of fusion increases. It, in turn, increases the frozen layer grown onto the additive in order to balance the conductive heat needed by the additive. Consequently time taken $\tau^*_{\max}$ to grow the frozen layer to its maximum extent, its melting time τ^*_{mel} and total time of freezing and melting τ^*_t increases.

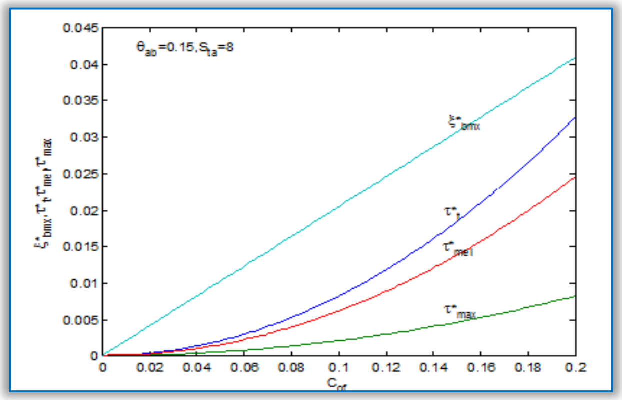

Figure 5 : Conduction factor, C_{of} dependent maximum frozen layer thickness, ξ^*_{bmx} , its growth time τ_{max} and the total time of the freezing and melting of the bath material τ_t, for prescribed θ_{ab} and S_{ta}.

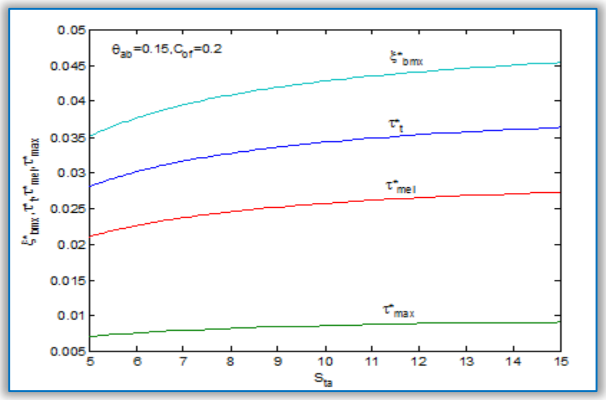

Figure 6:– S_{ta} variant maximum frozen layer thickness, ξ^*_{bmx} , its growth time τ^*_{max} and the total time of the freezing and melting of the bath material τ^*_t. C_{of} and θ_{ab} are employed as parameters.

Effect of Stefan number of the additive, S_{ta} :

Shown in Figure(3) time variant freezing and melting of the bath material ξ^*_{bm} onto the plate additive and melting and heating of the additive for different Stefan number S_{ta} of the additive. The C_{of} and θ_{ab} are considered as parameters. The behavior of these are similar to those appeared in the Figure(2). However, the size of the parabola decreases with increasing S_{ta}. It is against decreasing C_{of}. This features seems to be correct since increasing S_{ta} increases the sensible heat requirement as well as total heat requirement which can be compensated by bath convective heat due to which larger frozen layer thickness developed.Stefan number S_{ta} of the additive variant maximum frozen layer ξ^*_{bmx} developed, its time of formation, $\tau^*_{\max}$, its melting time, τ^*_{mel} and total time τ^*_t of freezing and melting are drawn for prescribed θ_{ab} and C_{of}. It is found increasing S_{ta} increases all these. Physically, it is true because raising the value of S_{ta} decreases the value of initial temperature θ_{ai} of the additive due to which the sensible heat requirement increases increasing the total heat i.e. the sum of sensible heat and latent heat of fusion of the additive. For thermal equilibrium, this heat needs to be supplied by the bath. Since bath convective heat is un–altered, more latent heat of fusion of the bath material is needed. It is compensated by growing large thickness of frozen layer that takes more time to grow, $\tau^*_{\max}$, its melting time, τ^*_{mel} and total time τ^*_t of freezing and melting also rises , Figure(6).

ISSN 1584 – 2665 (printed version); ISSN 2601 – 2332 (online); ISSN-L 1584 – 2665

Influence of melt temperature ratio, θ_{ab} :

Figure(4) exhibits freezing and melting of bath material ξ^*_{bm} onto the plate additive and melting and heating of the additive for various melt temperature ratio, θ_{ab}. Stefan number S_{ta} of the additive and conduction factor, C_{of} are taken as parameters. The features of the graphs are similar to those appeared in the Figure(2). When θ_{ab}, is allowed to decrease the parabola denoting freezing and melting of bath material gets smaller.

Figure(7) relates melt temperature ratio, θ_{ab} dependent maximum frozen layer grown ξ^*_{bmx}, its formation time, $\tau^*_{\max}$ its melting time, τ^*_{mel} and total time τ^*_t of freezing and melting for prescribed C_{of} and S_{ta}. The Figure(7) indicates that all of them have increasing trend once θ_{ab} is allowed to increases. These behaviour seems to be true as increasing θ_{ab} is caused by decrease in initial temperature, θ_{ai} of the additive. It results in providing more sensible heat which, in turn, increases the total heat i.e. the sum of sensible heat and latent heat of fusion of the additive. To balance it, a larger thickness of frozen layer is to be developed that takes larger frozen layer time $\tau^*_{\max}$, its melting time τ^*_{mel}. Consequently, the total time of freezing and melting τ^*_t also increases.

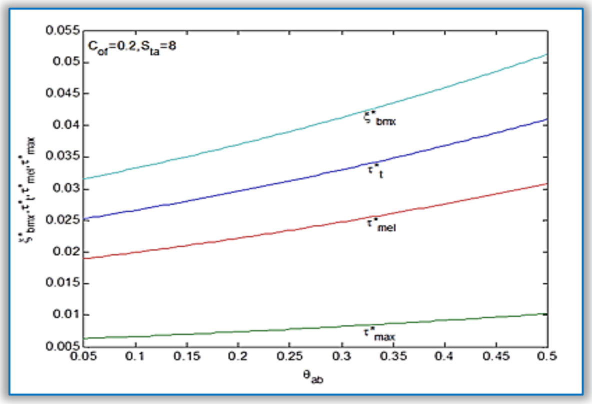

Figure 7: Variation of maximum frozen layer thickness, ξ^*_{bmx}, its growth time $\tau^*_{\max}$ and total time of freezing and melting of the bath material τ^*_t, C_{of} and S_{ta} are assumed as parameters.

6. CONCLUSIONS

In the present study, non–dimensional lump integral model devised for freezing and melting of an agitated bath material onto a low melting temperature plate additive gives close–form solutions for freezing and melting of bath material, ξ^*_{bm}, associated heating, ξ^*_{ai} and melting ξ^*_{am} of the plate additive in terms of conduction factor, C_{of}, phase–change parameter, the Stefan number, S_{ta}, of the additive and melt temperature–ratio, θ_{ab}. It is also observed that freezing time of the bath material is three times of the melting time of the frozen bath material. Decreasing any one of C_{of}, S_{ta} and θ_{ab} diminishes all these ξ^*_{bm}, ξ^*_{ai} and ξ^*_{am}. Solutions are validated by converting them to those of literature.

Nomenclature:

- B — property ratio, (K_bC_b/K_aC_a)
- B_i — Biot number, $h\, l_s/K_a$
- B_{im} — Modified Biot number, $(h\, l_s/K_a)*(K_aC_a/K_bC_b)$
- C — heat capacity $(\rho\, C_p)$, $Jm^{-3}K^{-1}$
- C_p — specific heat, $(J\,Kg^{-1}K^{-1})$
- C_r — heat capacity ratio, C_b/C_a
- h — heat transfer coefficient, $Wm^{-2}K^{-1}$
- K — thermal conductivity, $Wm^{-1}K^{-1}$
- L — latent heat of fusion, JKg^{-1}
- l_s — Significant length of the additive, (v/A_s)
- b — Semi thickness of plate, m
- ξ_{ah} — non–dimensional heat penetration depth in the additive, (x_{ah}/l_s)
- ξ_{ai} — non–dimensional heat penetration front in the additive at any time, (x_{ai}/l_s)
- ξ_{bf} — non–dimensional thickness within the frozen layer region, $(C_bx_{bf}/C_a\,l_s)$
- ξ_{bm} — non–dimensional thickness of the frozen layer front at anytime, $(C_bx_{bm}/C_a\,l_s)$
- S_{ta} — Stefan number of the additive, $C_a(T_{am}-T_{ai})/L_a\,\rho_a$
- S_{tb} — Stefan number of the bath material, $C_b(T_{bm}-T_{ai})/L_b\,\rho_b$
- t — time, s
- T — temperature, K
- T_b — bulk temperature of the bath material, K
- T_e — Equilibrium temperature at the interface between the additive and the frozen layer, K
- v — volume of the additive, m^3
- x — Frozen layer thickness, m

Greek Letters

- α — thermal diffusivity, $m^2 s^{-1}$
- ρ — density, (Kgm^{-3})
- θ — non–dimensional temperature, $(T-T_{ai}/T_{bm}-T_{ai})$
- τ — non–dimensional time, $(K_bC_b/C_a^2\,l_s^2)t$

Subscripts

- a — plate additive,
- a_i — initial condition of additive,
- a_f — within melting or freezing region of additive,
- a_h — within heating region of additive,
- a_m — melting or freezing of additive,
- b — frozen bath material or bulk condition of bath material,
- b_f — within melting or freezing region of bath material,
- b_m — melting or freezing condition of bath material,

ISSN 1584 – 2665 (printed version); ISSN 2601 – 2332 (online); ISSN-L 1584 – 2665

References:

[1] Singh U.C., Prasad A., .Kumar A., Acta Metallurgica Slovaca, 2013, Vol.19, No.1, pp. 60–72.
[2] Singh U.C., Prasad A., .Kumar A., J. Min. Metall, Sect B– Metall, 2012, Vol.48 (1) B, pp.11–23.
[3] Zhang L, Steel Res., 1996 Vol.67, No.11, pp.466–72.
[4] Prasad S., Prasad A., Kumar A.,, Annals of Faculty Engineering, Romania, May2018, pp53–66.
[5] Singh R.P., Prasad A., In the proceeding of the 7th European Oxygen Steel making Conference Trinec, Czech Republic, 2014, Sept.9–11.
[6] O.P.J. Gonzale, Macro A. Ramirez–Argaez and A.N.Corejo, ISI Journal International, Vol 50, 2010, No.1, pp 9–16.
[7] P.G.Sismansis, S.A.Arigyropaules: Canadian Metallurgical, Quarterly, Vol.72, 1988, p. 123
[8] R.P.Singh, A.Prasad: Vol. 37, 2003, p. 849–862.
[9] S.Sanyal, S.Chandra, S.Kumar, G.G.Roy: Vol.44, 2004, No. 7, p. 1157–1165.
[10] J.Li, G.Brooks, N.Provatas: Metallurgical and Materials Transaction B, Vol. 36B, 2005, p. 293–302.
[11] L.Pandelaers, F.Verhaeghe, D.Barrier, P.Gardin, P. Wollants, B. Blanpain: Ironmaking and Steelmaking, Vol. 37, 2010, p. 516–521.
[12] L.Pendelaers, F.Verhaeghe, B.Blanpain, P.Wollants and P.Gardin: Metallurgical and Materials Transaction B, Vol. 40B, 2009, p.676–684.
[13] Q.Jiao, N.J.Themelis: Canadian Metallurgical Quarterly, Vol. 32, 1993, p. 75–83.
[14] E.Rohmen, T.Bergstron, T.A.Engh: INFACON, Trondheim, Norway, 1995, p. 683–695.
[15] R.Kumar, S.Chandra, A.Chattrjee: Tata search, 1997, p.79–85.
[16] S.Taniguchi, M.Ohmi, S.Ishiura, S.Yamauchi: Trasactions ISIJ, Vol. 23, 1983, p. 565–570.
[17] S.Taniguchi, M.Ohmi, S. Ishiura: Transactions Iron and Steel Institute of Japan, Vol. 23, 1983, p. 571–575.
[18] B.K.Li, X.F.Ma, X.R.Zhang, J.C.He, Acta Metallurgica Sinica, Vol. 12, No.3, 1999, p. 259–266.
[19] U.C.Singh, A.Prasad, A.Kumar: Acta Metallurgica Slovaca, Vol. 19No. 1, 2013, p. 60–72.
[20] U.C.Singh, A.Prasad, A.Kumar: Journal of Mining and Metallurgy Section B, Vol. 48, No.1B, 2012, p.11–23.
[21] L.Zhang: Steel Research, Vol. 66, No.11, 1996, p. 466–472
[22] U.C.singh, A.Prasad, A.Kumar: Metallurgical and Materials Transaction B, Vol. 42B, 2011, p. 800–806.
[23] S.Prasad, A.Prasad, A.Kumar: Metallurgical and Materials Transaction B, Vol.46B, 2015, No.3, p.2616–2627.
[24] R.P.Singh and A.Prasad: Ironmaking and steelmaking, Vol. 32, 2005, p. 411–417.
[25] A. Prasad, S.P. Singh: Transaction. ASME, Vol. 166, 1994, p. 218–223.
[26] B.T.F.Chung, L.T.Yeh: Journal space craft, Vol.12, No.6, 1975, p. 329–333.
[27] L.T.Yeh, B.T.F.Chung: Journal space craft, Vol.14, No.3, 1977, p. 178–182.
[28] T.J. Lardner: AIAA Journal, Vol.5 No.11, 1967, p.2079–2080.
[29] A. Prasad: J. Spacecraft and Rockets: Vol. 16, 1979, p. 445–448.
[30] T.G.Myers, S.L.Mitchell, G.Muchabibaya, M.Y. Myers: International Journal Heat Mass Transfer, Vol.50, 2007, p.5303–5317.
[31] H.S.Carslaw, J.C. Jeager: Oxford University press, N.Y., 1959, p.72.
[32] E.R.G. Eckert and R.M.Drake, 'Analysis of Heat and Mass Transfer.' McGraw Hill Book Co. Tokyo, 1972.
[33] www.periodictable.com

ISSN 1584 – 2665 (printed version); ISSN 2601 – 2332 (online); ISSN–L 1584 – 2665